Contr. Mineral. and Petrol. 38, 21—36 (1973)

Experimental Deformation of Single Crystals of Biotite

M. A. Etheridge*, B. E. Hobbs**, and M. S. Paterson

Department of Geophysics and Geochemistry, Australian National University
Canberra, A.C.T. Australia

Received September 5, 1972

Abstract. Single crystals of biotite have been shortened up to 20% in compression tests parallel to [100], [110] and [010] directions at 3 Kbar confining pressure and temperatures from 300 to 700° C, and at a strain rate of 10^{-4} sec^{-1}. Thick metal constraining sleeves were used and led to a distribution of kinking throughout the crystals. The orientation of kink boundaries, angle of bending and asymmetry of the basal plane across the kink boundaries and the axes of bending were measured. A minor amount of unidentified non-basal slip must have occurred to account for the assymmetry, but basal slip predominates at all temperatures. From the axes of bending, the discrete slip directions [100], [110] and [1$\bar{1}$0] for basal slip are deduced. Increase in temperature mainly leads to a simpler pattern of kinking associated with the kinks being wider and the kinking angle larger, presumably as a result of greater mobility of dislocation walls that form the kink boundaries.

Introduction

It is generally accepted that slip occurs on the (001) plane in micas, but the slip direction is less certainly known. From the observation that cleavage occurs at the plane of the potassium atoms (e.g. Bragg and Claringbull, 1965, p. 259 and 266), it may be expected that the slip will alsoc occur at this layer in the unit cell. Then, by analogy with metallic and ionic crystals (e.g. Honeycombe, 1968, p. 11), one would predict that the slip directions will be the directions of closest packing of the potassium atoms, that is, [100], [110] and [1$\bar{1}$0]. The repeat distances in [100] and in the two equivalent ⟨110⟩ are the same if $a:b=1:\sqrt{3}$, as is almost exactly the case in both biotite and muscovite. Therefore, slip in all three directions should occur with almost equal facility since more distant neighbour interactions are unlikely to have any significant effect.

The experimental observations so far on slip directions have not given consistent or conclusive verification of these predictions. From "pressure" and "percussion" figures, Mügge (1898; see also Friedel, 1926, p. 506) concluded that the (001) slip in mica probably did occur in the directions [100] and [110], these directions being normal to the observed axes[1] of bending or kinking. Also, Borg

* Now: Department of Geology and Mineralogy, University of Adelaide, Adelaide, South Australia.

** Now: Department of Earth Sciences, Monash University, Clayton, Victoria.

1 In his summary table, Mügge lists these axes as [010] and [130] but the latter seems to be quoted in error, and in conflict with his text, in place of [310]. Borg and Handin (1966) have quoted the [130] indices as given by Mügge in his table. In the analysis of their own observations there has been a confusion between direction indices and plane normal indices. When this is corrected, their results would also indicate [100] and [110] as active slip directions in [001] (Borg, private communication).

and Handin (1966) found some indications for slip parallel to [110] as well as [100], but they only loaded crystals in one orientation (compression in a direction in the (100) plane, nearly halfway between [100] and [110]). On the other hand, Hörz and Ahrens (1969, 1970) concluded from studies of kinking in shock-loaded biotite that there is no crystallographic control on the slip directions within (001). Yet in a brief comment on electron microscopic observation of dislocations lying in the basal plane of muscovite, Amelynckx and Delavignette (1962) point out that the dislocations are undissociated and that the Burgers vectors connect the potassium atoms, presumably implying [100] and ⟨110⟩ slip directions.

The question of the slip system is only one aspect of the study of deformation in micas. The singular slip plane also results in an extreme plastic anisotropy which in most practical situations leads to a profusion of kinking; the kinking in part overcomes the limitation of uniform basal slip in achieving a general deformation (Paterson, 1969). Therefore the study of kinking is an important aspect of deformation of micas, especially in relation to structural field studies.

In the present study, biotite crystals have been compressed parallel to the basal plane in three different directions and over a range of temperatures. The aim has been partly to throw further light on the crystallography of slip, especially on the slip direction, and partly to observe the influence of temperature on the kinking patterns. The specimens have been constrained in thick metal jackets in order to avoid excessive localization of the deformation and to simulate natural situations more closely and make the study more geologically relevant.

Experimental Details

Specimens were taken from a large (approx. $30 \times 20 \times 15$ cm) single crystal of biotite from Mt. Isa, Queensland, Australia. The biotite is deep red-brown in hand specimen, and pleochroic straw-yellow to dark-brown in thin section with a 2 V of 10°. It shows no significant signs of previous deformation but contains 10–20% white mica in elongate inclusions parallel to (001). Using Laue photographs taken normal to (001) to orient the crystal, cores of 7 mm diameter and 15 mm length were obtained parallel to [010], [100] and [110] with a diamond coring drill. In most cases, the specimens did not part along (001) during the coring. The cores were then enclosed in thick stainless steel jackets of 10 mm external diameter (in one case, TZM molybdenum alloy from Climax Molybdenum, U.S.A. was used instead). The composite specimen was sealed from the argon pressure medium by a thin annealed copper jacket. The apparatus, specimen arrangement and testing procedure have been described elsewhere (Paterson, 1970).

Five experiments were carried out to 20% shortening in each of the three orientations, from 300 to 700° C. Also a few experiments were done at smaller strains (2–10%) at 700° C in the [100] orientation. All experiments were done at 3 Kbar confining pressure and at a strain rate of approximately 10^{-4} sec^{-1}.

After deformation, the specimens were impregnated with an epoxy resin and thin sections were then prepared normal to the mean attitude of (001) and parallel to the specimen axis. The orientations of 50 typical kink boundaries and of (001) on each side of each boundray were determined in each specimen using a four-axis universal stage.

In deriving the stress-strain curves of the biotite, load measurements obtained with an internal load cell were used and the load supported by the thick metal jackets was subtracted. The latter was obtained from two sequences of runs, under the same conditions as the biotite runs, on dummy specimens, one sequence using 7 mm diameter annealed copper inside the steel (or molybdenum) jackets and the second using unsleeved annealed copper specimens of 10 mm diameter. The calculated stresses are based on "actual" cross-sectional area during straining (assuming no barelling and no volume change). In view of the large corrections

arising from the strength of the thick metal jackets being several times that of the biotite, and in view of the heterogeneity that develops during straining (including at the ends of the composite dummy specimens), the resulting stress-strain curves are of rather low accuracy, especially at large strains; however, the reporducibility at strains of 5% is roughly within 10%.

Experimental Results

Stress-Strain Results

The stress-strain curves for the constrained biotite crystals loaded parallel to [010] at 400, 600 and 700° C are shown in Fig. 1; the curves for 300 and 500° C were similar to that for 400° C, there being only slight weakening accompanying increase in temperature in this range. The curves for [100] and [110] orientations were similar but often slightly lower than for the [010] orientation; however, the difference in yield stress is rarely greater than 10% and so, in view of the comments on accuracy above, may not be significant. Thus the yield stresses are an order of magnitude higher than the values (70–80 bars) observed by Borg and Handin (1966) at 500° C and 5 Kbar for an orientation intermediate between [100] and [110], presumably mainly due to differences in lateral constraint.

Specimen Shape

After deformation, all the specimens are elliptical in the section normal to the axis of shortening, with the major axis normal to intersection of (001). As gauged from the outside dimensions of the thick matal jacket after deformation, this major cross-sectional diameter has increased in length by 20–25%, whereas the minor diameter, parallel to the trace of (001), has remained unchanged within 5%. This suggests that slip has been confined to slip directions approximately normal to the minor diameter, although probably any increase in minor diameter

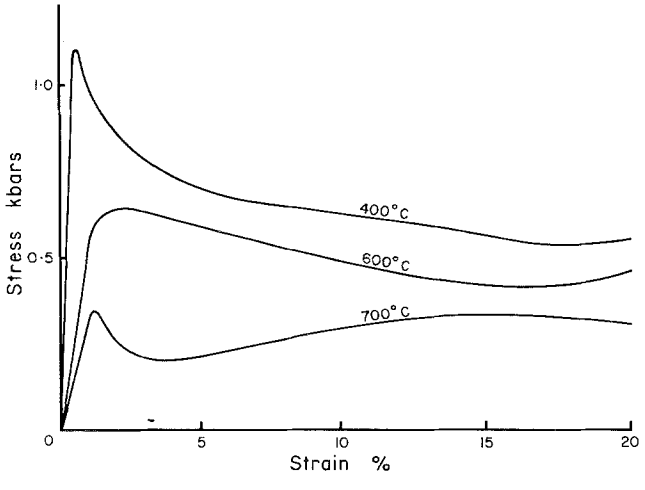

Fig. 1. Stress-strain curves for biotite single crystals compressed parallel to [010] direction in steel constraining jacket (corrected for strength of jacket). At 300 and 500° C, the curves are very similar to that at 400° C, with a small decrease in strength with increasing temperature

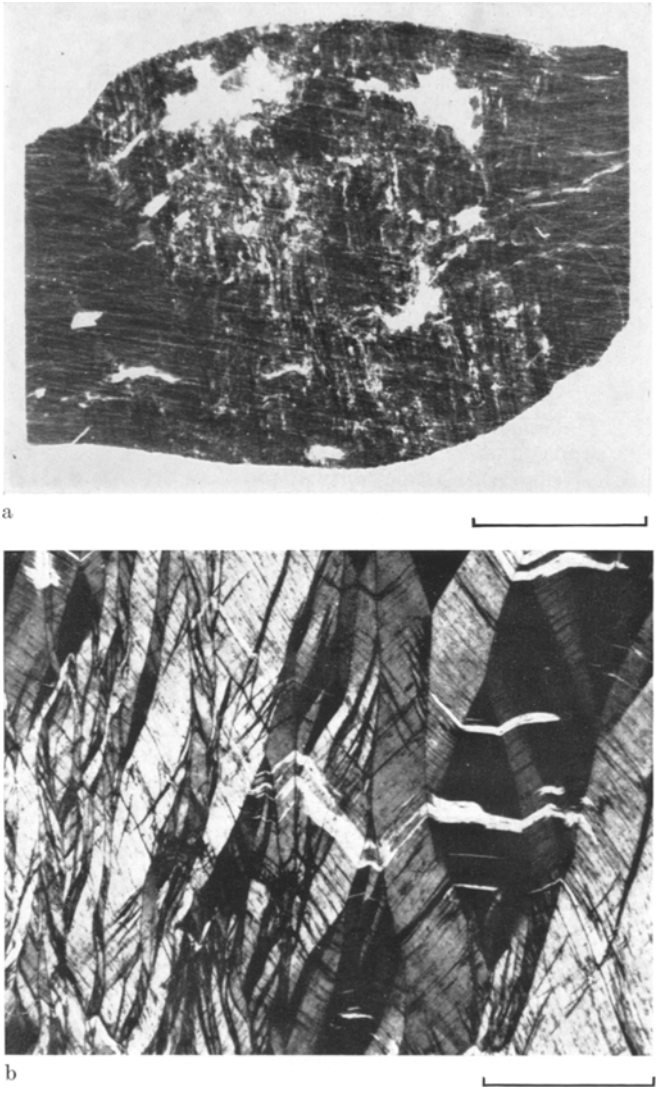

Fig. 2. (a) Asymmetric barrelling of specimens, as shown in section normal to (001) plane and parallel to shortening direction (strained 20% at 700° C). (b) Distribution of kinks in centre of specimen shortened 20% parallel to [100] direction at 300° C. Scale bar is 400 μm long. (c) Distribution of kinks in centre of specimen shortened 20% parallel to [100] direction at 700° C. Scale bar is 400 μm long. In each case, compression axis is horizontal and crossed polarizers are used

associated with slip in ⟨110⟩ directions in the [010] specimens would have been undetected.

In the plane of the thin section, the profile shows the usual barelling associated with frictional end constraint (Fig. 2a). However, in addition, all the specimens

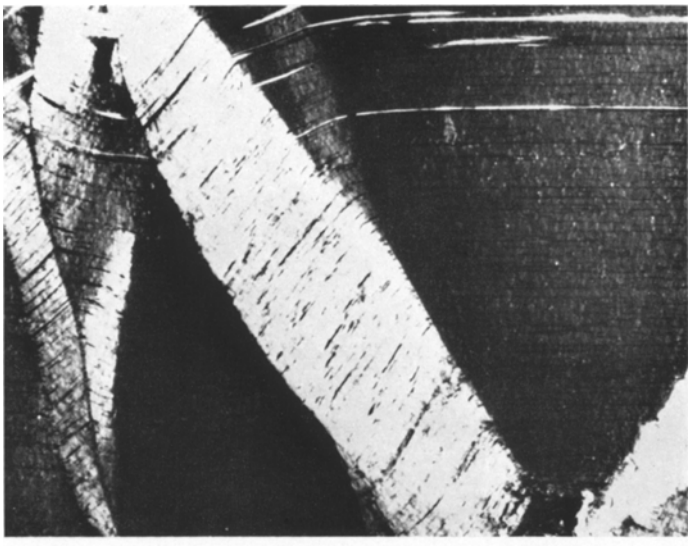

Fig. 2c

became asymmetrical except one [010] specimen at 700° C and one [100] at 300° C. There is no apparent temperature or specimen orientation control over the occurrence or the degree of this asymmetry of barelling.

Description of Structures

The thin sections show that the main product of the deformation is a multiplicity of kinks and related structures. The kinks are widely distributed throughout the specimens as a result of the strong lateral constraint which inhibits a concentrated local development like that in the relatively unconstrained specimens of Borg and Handin (1966; compare their plates 1A and B with our Fig. 2a). The behaviour of the constrained specimens is therefore more nearly similar to that of a crystal of mica in an aggregate (cf. the crystal from a deformed diorite shown by Borg and Handin, 1966, plate II).

The geometrical properties of the kinks, described in detail below, vary with temperature but apparently do not depend significantly on the orientation of the compression axis in the basal plane. Where individual kink bands can be distinguished, their shape is extremely variable, ranging from small lensoid regions to broad kink bands with more or less parallel boundaries which can be traced across the specimen. The boundaries of the regions are rarely strictly planar and may change in orientation along their trace in the section, in extreme cases by up to 25°. The larger kinks (especially in the higher temperature specimens) either narrow rapidly along their length or die out into regions of gentle bending towards the margins of the specimen. Thus, there is rarely a sharp kink in the specimen boundary or the steel jacket. At lower temperatures, the kink bands tend to be narrow, short (rarely longer than 1 mm), curved regions which closely interfinger (Fig. 2b) such that undeformed ragions are rare. In the less-deformed

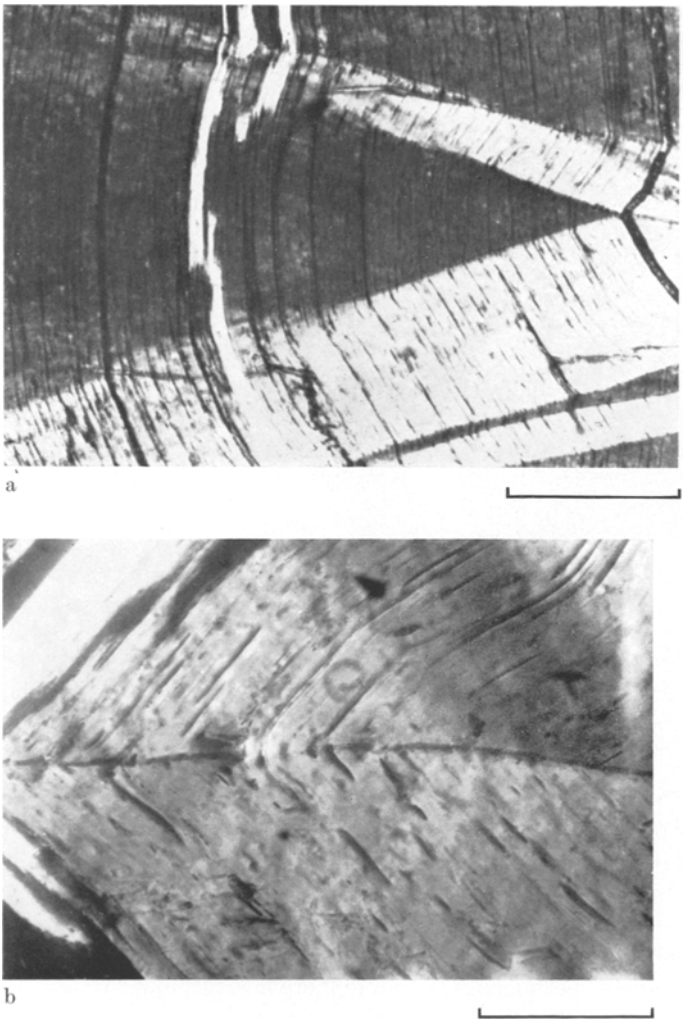

Fig. 3. (a) Kink on concave side of a region of bending, in opposite sense to proposed mechanism of Mügge (1898), at 600° C. Scale bar is 100 μm long. (b) Optically resolved region of bending in a high angle kink, at 700° C. Scale bar is 30 μm long. (c) Fine second generation kinks within secondary kink bands in a specimen shortened 20% parallel to [100] at 400° C. Scale bar is 100 μm long. In each case, compression axis is vertical and crossed polarizers are used

end regions of most specimens, the particular type of structure shown in Fig. 3a is found; it occurs on the concave side of a region of bending of (001) but involves an opposite sense of kinking to that described by Mügge (1898).

The practical analysis of kinks tends to concentrate on the kink boundaries. Weiss (1969, p. 306) has distinguished between "*primary*" and "*secondary*" kink boundaries according to whether the slip associated with the kinking process has occurred on one side or on both sides of the boundary, respectively (any more

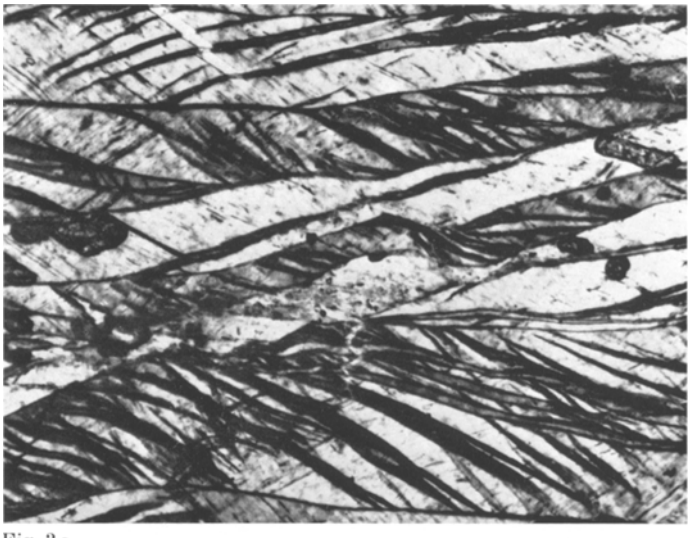

Fig. 3c

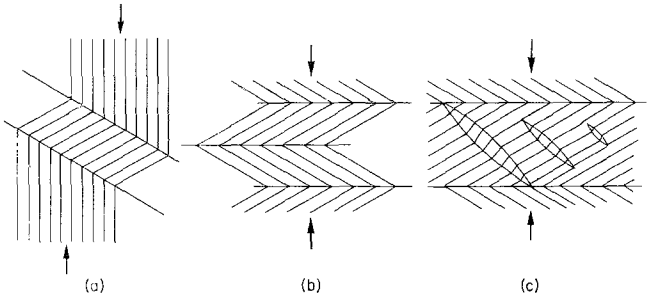

Fig. 4a—c. Sketch of various types of kink bands formed in these experiments. (a) Primary kink bands; (b) secondary kink bands; (c) second generation kink bands. Arrow indicate compression direction

or less homogeneous shearing affecting both areas prior to the development of the kink is ignored in this context). This distinction can often be made in the present specimens and in addition it is often possible to distinguish *primary kink bands*, in which both boundaries are of the primary type (Fig. 4a), and *secondary kink bands*, in which one or both boundaries are of the secondary type (Fig. 4b). It is also possible in some cases to distinguish *second generation kink bands*, for example bands analogous to primary kink bands but which occur wholely within material that has already been sheared in the formation of a primary or secondary kink band (Fig. 4c); cf. Weiss, 1969, plate 18D). However, in the complicated patterns of deformation that develop in the mica crystals after substantial strains (e.g. Fig. 2b), it is not always possible to decide whether a given kink boundary is of primary or secondary type, or even to distinguish individual kink bands as entities. Moreover, such distinctions tend to be even more difficult to make in

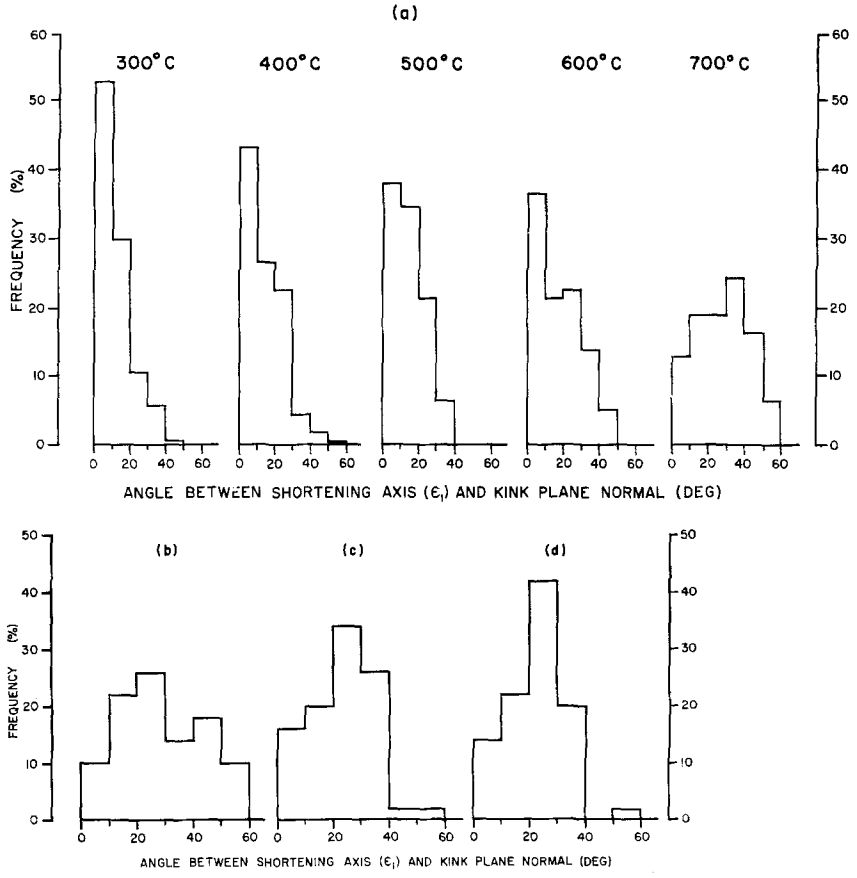

Fig. 5a—d. Frequency distributions of angles between shortening axis (ε_1) and normals to kink planes. (a) Influence of temperature (20% strain). All specimen orientations included in this diagram. 150 readings at each temperature. (b) 700° C in TZM molybdenum jacket (20% strain). [100] orientation. 50 readings. (c) 700° C, 2% strain, [100] orientation, 50 readings. (d) 700° C, 5% strain, [100] orientation, 50 readings

naturally deformed rocks. Therefore in what follows, all kink boundaries have been treated together except where implicit distinction between primary and secondary is mentioned.

The following are the results of detailed microscopic study of the kinking and its dependence both on orientation and on temperature:

1. Geometrical Characteristics

In the specimens shortened 20%, the kinks become less numerous, broader and less highly inclined to the direction of maximum shortening (ε_1) as the temperature increases. At 300 to 500° C, there is a concentration, in the central region of the specimen, of narrow kinks, 0.01–0.2 mm in width, inclined at high angles (70–90°) to ε_1, with almost no intervening areas where the initial orientation of (001) is

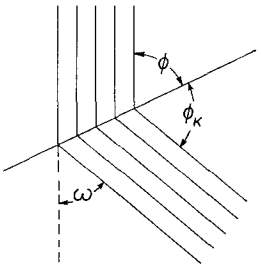

Fig. 6. Sketch showing angle designations

unchanged (Fig. 2b). However, at 600° and, more so, at 700° (Fig. 2c), the centra region of the specimen contains greater undeformed areas and the kinks are broader (0.05–0.5 mm in width), are less highly inclined to ε_1 (30–70°) and can often be traced right across the specimen. The change in inclination of kink boundaries with temperature is shown in Fig. 5a and is seen to be most marked between 600 and 700° C. It probably reflects, in part, an increase in relative preponderance of primary over secondary kink boundaries.

The experiment, at 700° C, with the molybdenum alloy jacket yielded similar kink boundary orientations to the comparable experiment with stainless steel jacket (Fig. 5b) although the degree of lateral constraint is different. The molybdenum alloy jacket at 700° C has comparable strength to the stainless steel at 300° C, although its constraining effect will be rather less because it has a lower rate of work-hardening. However, in neither case do the kinks impinge on the jackets in such a way as to cause extensive local deformation, suggesting that the constraint is highly effective in both cases. Thus we conclude that the above changes in character of the kinking with temperature can be ascribed to the influence of temperature on the intrinsic behaviour of the biotite and not simply to a change in the degree of constraint.

The progressive development of kinking was examined in several experiments with the [010] orientation at 700° C, straining up to 2 and 5% shortening. At 2%, a few small kinks (up to 20 μm wide) had formed, the boundaries of which had the orientations shown in Fig. 5c. An increase to 5% shortening gave rise to a similar number of wider kinks of almost identical orientation (Fig. 5d). At 20% shortening (Fig. 2a), the kink bands are again wider, while the range of orientations although a little broadened, is still generally similar. These observations suggest that the amount of shear within each kink band does not change markedly with progressive shortening; rather, strain is taken up to a large entent by enlargement of the bands and the formation of some new ones.

In some specimens, especially those which show distinctly asymmetric barrelling, a large number of fine kinks (5 to 50 microns in width) are found wholly within a single larger kink band (Figs. 2b and 3c). These second generation kinks occur predominantly in kink bands of one sense of rotation in a given specimen, related to the sense of asymmetric barelling (cf. Fig. 2a).

The *angle of bending*, ω, of the basal plane across a kink boundary (Fig. 6) is rarely less than 25° or more than 120° but is widely distributed between (Fig. 7). The apparent insensitivity of this range to change in temperature when all kink boundaries are treated together masks an influence of temperature on

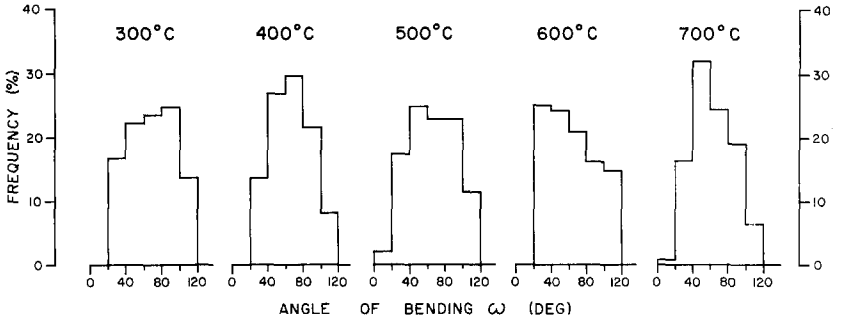

Fig. 7. Frequency distributions of the angle of bending of (001) plane across a kink boundary (ω) at various temperatures. All specimen orientations included. 250 readings each

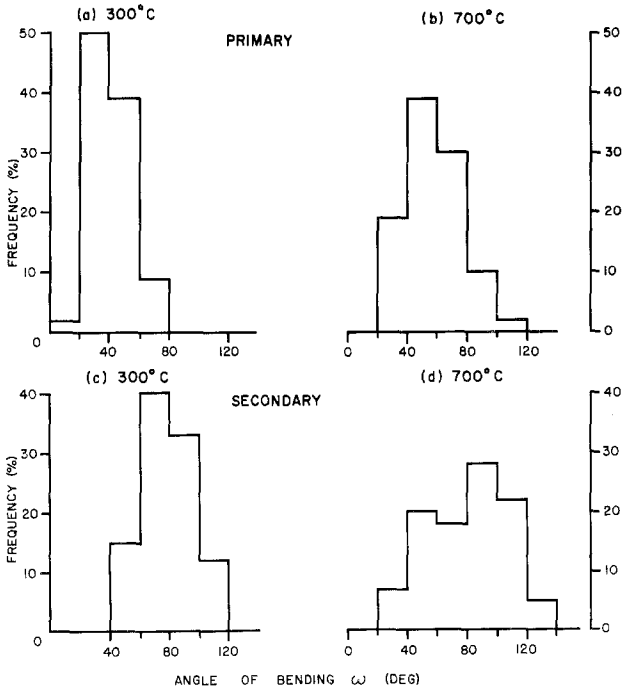

Fig. 8a—d. Frequency distributions of the angle of bending of (001) plane across a kink boundary (ω) at 300 and 700° C. (a), (b) primary kink boundaries; (c), (d) secondary kink boundaries; All specimen orientations included

the angle of bending at a particular type of boundary, owing to a change in the relative preponderance of primary and secondary boundaries. Distinguishing these as well as is possible leads to the results in Fig. 8, where Figs. 8a and b give values of ω at primary boundaries at 300 and 700° C, while Figs. 8c and d show the corresponding values for secondary boundaries. This suggests that there is a real increase in both mean value and spread of ω with increase in temperature.

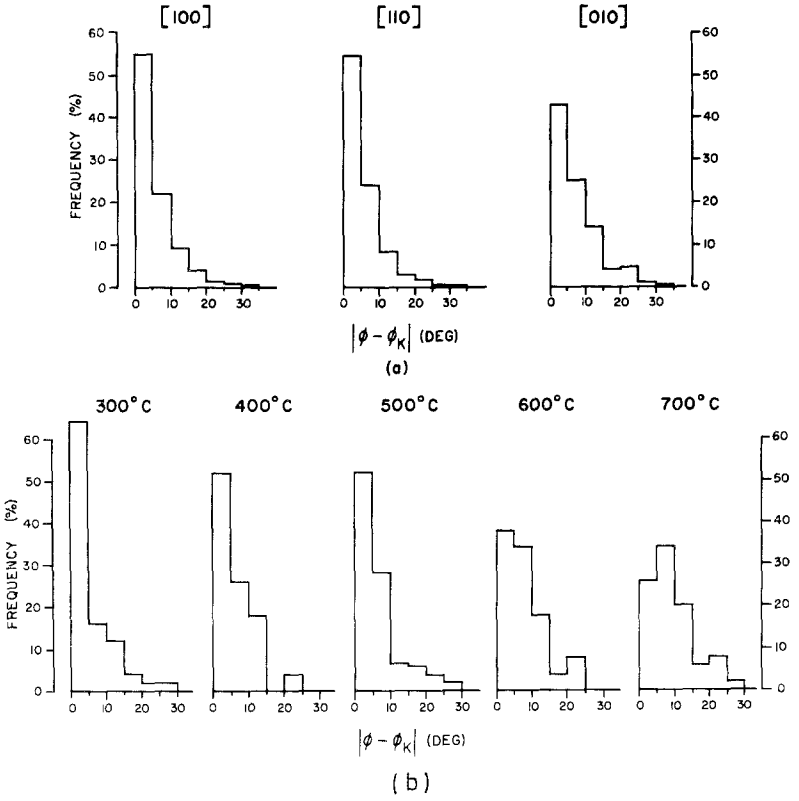

Fig. 9a and b. Frequency distribution of kink asymmetry ϕ–ϕ_k. (a) Influence of orientation. All temperatures included. 250 readings each plot. (b) Influence of temperature of [010] orientation. 50 readings each

The kink boundaries for which ω is less than about 45° C often change character along their length from a sharp kink to a zone of uniform bending (for example, Fig. 3a). In other cases, where ω is high, this transition from a planar structure to a region of curvature is quite sudden. A boundary of the latter type is shown in Fig. 3b; the angle of bending does not change markedly along this kink but the actual boundary changes character a number of times.

The *asymmetry* $|\phi$–$\phi_k|$ of inclination of the basal plane to the kink boundary (Fig. 6) is dependent on both temperature and specimen orientation (Fig. 9a and b) but is the same for both primary and secondary boundaries. In [100] and [110] specimens the kink boundaries tend to be nearly symmetrical, although rare values of $|\phi$–$\phi_k|$ up to 30° are recorded, while in the [010] specimens there seems to be rather less tendency to symmetry, the arithmetic means of $|\phi$–$\phi_k|$ being 5°, 5° and 7°, respectively, for [100], [110] and [010] orientations. Where the asymmetry is beyound doubt, say, ϕ–$\phi_k > 10°$, the larger inclination to the boundary showed no preference for the deformed or undeformed side where the boundary could be distinguished as a primary one. Increasing the temperature

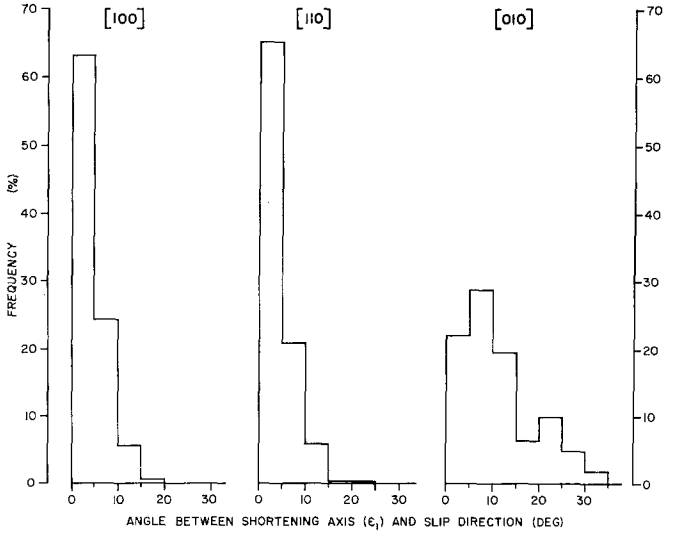

Fig. 10. Freqeuncy distribution of the angle between the specimen axis and the slip direction for different orientations. All temperatures are included. 250 readings each

tends to increase the degree of asymmetry in the case of the [010] orientation (Fig. 9b) but not to change it significantly in the [100] and [110] cases.

Measurement of the orientation of the basal plane on both sides of a kink boundary as well as of the kink boundary itself enables one to show that all three intersect in the same line, which is the *axis of rotation* associated with the kinking. Assuming the basal plane to be the only active slip plane, the resultant slip direction is then the line within it which is normal to the axis of rotation. Fig. 10 gives results of determination of "slip direction" made in this way, its orientation being expressed by the angle by which it deviates from the line initially parallel to the specimen axis. The deviation is small (mean 4°) in specimens compressed parallel to [100] and [110], suggesting that basal slip is favoured parallel to these two directions, whereas the deviation tends to be much greater (mean 11°) for the [010] specimens, suggesting that [010] is not a favoured slip direction; presumably in the latter case, the resultant slip directions are irrational ones resulting from a variable relative contribution from slip in the [100] and [110] directions.

2. Optical Characteristics

The kink boundary is generally a well-defined plane which can be brought into sharp focus on the universal stage. The apparent width of its image does not exceed the resolving limit of the objective at moderate magnifications, but it does when the numerical aperture (N.A.) exceeds 0.50. The measurements in Table 1 suggest that the boundary width is of the order of 1–2 μm. When it is viewed in the vertical position in bright-field illumination with the condenser aperture stopped down and the top surface of the thin section is focused upon, the

Table 1

Lens magnification	Numerical aperture	Apparent object width (μm)	
		Calculated[a]	Measured
× 10	0.22	3,0	2.8
× 25	0.50	1.3	1.7
× 45	0.65	1.0	1.6
× 100 (oil)	1.25	0.5	1.7

[a] From theory of McLaren *et al.* (1970) for a phase object of real width ≈ 0.2 μm or less.

boundary appears as a dark line with a weak bright fringe on either side; this contrast is reversed when the lower surface is focussed upon, and there is minimal contrast when the central part of the section is in focus. Such behaviour indicates that the boundary is behaving as a phase object, although the out-of-focus image contrast is the reverse of that discussed by McLaren, Turner, Boland and Hobbs (1970). This suggests that the relative change in refractive index in the boundary region is opposite to that in the lamellae in synthetic quartz studied by McLaren *et al.* (op. cit.).

As is usual in thin sections of mica, there are many discretely visible planes parallel to (001) which are presumed to be cleavages. Their distribution and clarity does not vary noticeably inside and outside kink bands, however, contrary to the observation of Borg and Handin (1966, p. 277). The best defined visible (001) surfaces continue across kink boundaries but there are also many which terminate at boundaries, both from outside and from inside a kink band. Visible separation at the (001) surfaces is rare and is only seen at the termination of markedly elliptical kinks.

Discussion

Mechanisms

Our observations are consistent with (001) being the dominant slip plane up to at least 700° C since this plane is fairly symmetric with respect to the kink boundaries over the whole temperature range. Further, the measurements of axes of bending associated with the kinking indicate that in the (001) plane there are well-defined slip directions [100] and ⟨110⟩ (cf. Introduction). Our observations do not support the conclusion of Hörz and Ahrens (1969, 1970), based on shock experiments, that there is no crystallographic control on the slip direction in (001).

The geometry of slip in the [010] specimens can be interpreted as follows: If the resistance to slip in a given direction is assumed to be proportional to the square of the Burgers vector b for that slip direction, then the resistance to slip parallel to [010] should be three times that for slip parallel to [100] and ⟨110⟩ since

$$b_{[010]} = \sqrt{3} \cdot b_{[100]} = \sqrt{3} \cdot b_{\langle 110 \rangle}.$$

However, in the specimens compressed parallel to [010] in which kinking occurred with a kink axis approximately normal to the axis of loading and in which therefore

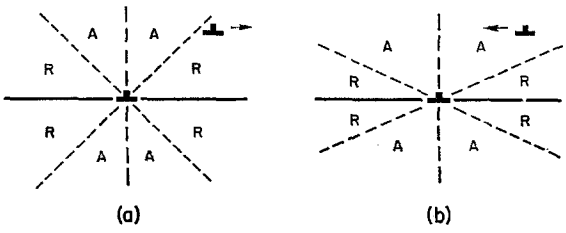

Fig. 11. Force fields around a dislocation, showing regions where a second like dislocation is attracted (A) and repelled (R). After Chou (1962). (a) Isotropic crystal. (b) Strongly anisotropic crystal

the maximum resolved shear stress in the (001) plane in the kink will be approximately parallel to the [010] direction, this resolved shear stress will not exceed by three times the resolved shear stress parallel to [110] and [1$\bar{1}$0]. Therefore, we can expect [110] and [1$\bar{1}$0] slip to occur in preference to [010] slip, the resultant shear in approximately the [010] direction being achieved by a combination of [110] and [1$\bar{1}$0].

The degree of asymmetry observed at some kink boundaries indicates that some mechanism other than basal slip must also be active to a minor extent. Asymmetry of about 5° has previously been reported by Borg and Handin (1966) in experimentally deformed biotite and by Turner (1964) in naturally deformed mica, while values of 10 and even as high as 32° have been found in experimentally and naturally shocked material (Hörz and Ahrens, 1969; Hörz, 1970). Such asymmetry cannot be accounted for by elastic strain on the scale of the kink bands. For example, a uniform shear parallel to a kink boundary, in a direction normal to the kink axis, would have to be of magnitude $\frac{1}{2}\frac{\sin(\phi-\phi_k)}{\sin\phi\sin\phi_k}$ in order to produce an asymmetry of $\phi-\phi_k$; for typical values of ϕ and ϕ_k greater than 45°, this correspinds to a shear of 0.02 to 0.04 for $\phi-\phi_k=5°$. Elastic shears of this magnitude ore at least an order of magnitude greater than would correspond to the macroscopic stresses that mica is known from experiment to support. The observed asymmetry must therefore presumably be attributed to non-basal slip, which will contribute to the kink boundary region dislocations other than those for basal slip, these dislocations serving to accomodate the associated mis-match in crystal structure across the boundary. Climb of basal dislocations in itself could not give rise to the asymmetry.

Following Hess and Barrett (1952) and Washburn and Parker (1952), the kink boundary can probably be considered as a wall of dislocations of predominantly one sign, capable of moving laterally as the kink band widens during deformation. This would be consistent with the observations described above which show that kinks widen while maintaining an approximately constant angle of bending ω at their boundaries. It would also be consistent with the theory of Frank and Stroh (1952) according to which the widening of a kink nucleus in this way is only possible if the angle of bending at the boundary exceeds a certain value, which rough calculation suggests will be very small in mica. Such a dislocation array would be especially stable in mica because the strong elastic anisotropy gives rise to a larger sector above a given dislocation in which there is an attractive force on a like dislocation (Chou, 1962; see Fig. 11). However, since the observed

angles of bending are much larger than would correspond to single arrays of dislocations with spacing substantially larger than the lattice plane spacing, the kink boundary may have a more complex character than usually depicted. No discretely preferred values of ω were noted in support of the simple fit model of Starkey (1968). In addition, the measurements in Table 1 indicate that the boundary has a finite width of the order of 1–2 μm, supporting the idea of a complex structure.

Influence of Temperature on Kinking

The principal effect of an increase in temperature is to lead to wider kink bands and to a simpler over-all structure on account of there now being fewer intersections. Other effects such as changes in asymmetry are minor, suggesting that there is no marked influence of temperature on the slip mechanisms in the range studied. The pattern of wider kinks probably results from increase in temperature faciliating the migration and mutal intersection of the kink boundaries and reflects increased dislocation mobility and recovery rates.

Geological Significance

Kinks in mica have been used for deriving the principal stress directions in the late stages of rock deformation (e.g. Turner, 1964). Poles to kink boundaries tend to concentrate about a single maximum, which is identified as the direction of maximum principal compressive stress. However, there is generally considerable scatter in the distribution and the present experiments suggest that this is due, at least in part, to measurements on both primary and secondary kink boundaries being included. Primary kink boundaries can never form precisely normal to the loading direction, although the departure may not be large when ω is small; but there will tend to be a conjugate development of primary kinks in grains loaded symmetrically with respect to (001). Therefore, we suggest that a more precise location of the maximum principal compressive stress may be gained by considering only grains containing conjugate primary kinks and/or secondary kinks—the former being symmetrically disposed about (001) and the latter being normal to (001).

Acknowledgements. The work for this paper was supported by a Commonwealth Postgraduate Scholarship for M.A.E. We thank Mr. G. T. Milburn for preparation of the thin sections and other technical assistance, and Mr. A. W. Geatley for assistance in maintaining the apparatus.

References

Amelynckx, S., Delavignette, P.: Dislocations in layer structures. Proc. Tech. Conf. on Direct Observations of Imperfections in Crystals, Missouri, 295–356 (1962).

Borg, I., Handin, J.: Experimental deformation of crystalline rocks. Tectonophysics **3**, 249–368 (1966).

Bragg, Sir L., Claringbull, G. F.: Crystal structures of minerals. London: Bell 1965.

Chou, Y. T.: Width of an extended dislocation. Acta Met. **10**, 739–740 (1962).

Frank, F. C., Stroh, A. N.: On the theory of kinking. Proc. Phys. Soc. (London) B **65**, 811–821 (1952).

Friedel, G.: Leçons de crystallographie. Paris: Berger-Levault 1926.

Hess, J. B., Barrett, C. S.: Structure and nature of kink bands in Zn. Trans A.I.M.E. **185**, 599–606 (1949).

Honeycombe, R. W. K.: The plastic deformation of metals. London: Edward Arnold 1968.

Horz, F.: Static and dynamic origin of kink bands in micas. J. Geophys. Res. **75**, 965–977 (1970).

Horz, F., Ahrens, T. J.: Deformation of experimentally shocked biotite. Am. J. Sci. **267**, 1213–1229 (1969).

McLaren, A. C., Turner, R. G., Boland, J. N., Hobbs, B. E.: Dislocation structure of the deformation lamellae in synthetic quartz; a study by electron and optical microscopy. Contr. Mineral. and Petrol. **29**, 104–115 (1970).

Mügge, O.: Über Translationen und verwandte Erscheinungen in Krystallen. Neues Jahrb. Mineral. Geol. Paläontol. **1**, 71–158 (1898).

Paterson, M. S.: The ductility of rocks. Physics of strength and plasticity, A. S. Argon, ed., p. 377–392. Cambridge, Mass.: M.I.T. Press 1969.

Paterson, M. S.: A high-pressure, high-temperature apparatus for rock deformation. Int. J. Rock Mech. Min. Sci. **7**, 517–526 (1970).

Starkey, J.: The geometry of kink bands in crystals—a simple model. Contr. Mineral. and Petrol. **19**, 133–141 (1968).

Turner, F. J.: Analysis of kinks in mica of an Innsbruck mica schist. Neues Jahrb. Mineral. Monatsh. **9**, 51–83 (1964).

Washburn, J., Parker, E. R.: Kinking in Zn single-crystals tension specimens. J. Metals **4**, 1076–1082 (1952).

Weiss, L. E.: Flexural slip of foliated model materials. Proceedings of Conference on Research in Tectonics (Kinkbands and Brittle Deformation), Ottawa, March 1969, A. Baer and D. Norris, eds. Geol. Surv. Cam. Pap. 68–52 (1969).

Dr. M. A. Etheridge
Department of Geology and Mineralogy
University of Adelaide
Adelaide
South Australia